




Cite this: *RSC Adv.*, 2018, 8, 21065

# The physiological responses of terrestrial cyanobacterium *Nostoc flagelliforme* to different intensities of ultraviolet-B radiation†

Shi-gang Shen, Shi-ru Jia, Rong-rong Yan, Yi-kai Wu, Hui-yan Wang, Ya-hui Lin, Dong-xue Zhao, Zhi-lei Tan, He-xin Lv and Pei-pei Han \*

*Nostoc flagelliforme* is a pioneer organism in the desert and exerts important ecological functions. The habitats of *N. flagelliforme* are characterized by intense solar radiation, while the ultraviolet B (UV-B) tolerance has not been fully explored yet. To evaluate the physiological responses of *N. flagelliforme* to UV-B radiation, three intensities ( $1 \text{ W m}^{-2}$ ,  $3 \text{ W m}^{-2}$  and  $5 \text{ W m}^{-2}$ ) were used, and the changes in photosynthetic pigments, cell morphology, mycosporine-like amino acids (MAAs) synthesis and cell metabolism were comparatively investigated. Under high UV-B intensity or long term radiation, chlorophyll *a*, allophycocyanin and phycocyanin were greatly decreased; scanning electron microscope observations showed that cell morphology significantly changed. To reduce the damage, cells synthesized a large amount of carotenoid. Moreover, three kinds of MAAs were identified, and their concentrations varied with the changes of UV-B intensity. Under  $1 \text{ W m}^{-2}$  radiation, cells synthesized shinorine and porphyra-334 against UV-B, while with the increase of intensity, more shinorine turned into asterine-330. Metabolite profiling revealed the contents of some cytoprotective metabolites were greatly increased under  $5 \text{ W m}^{-2}$  radiation. The principal component analysis showed cells exposed to UV-B were metabolically distinct from the control sample, and the influence on metabolism was particularly dependent on intensity. The results would improve the understanding of physiological responses of *N. flagelliforme* to UV-B radiation and provide an important theoretical basis for applying this organism to control desertification.

Received 11th May 2018

Accepted 2nd June 2018

DOI: 10.1039/c8ra04024a

rsc.li/rsc-advances

## 1. Introduction

Cyanobacteria are primitive oxygenic bacteria, which probably appeared on the Earth about 3.5 billion years ago during the Precambrian era.<sup>1</sup> They have the ability to fix atmospheric nitrogen and thus play a significant role in turning desert into fertile soil.<sup>2</sup> It has been estimated that cyanobacteria fix over 35 million tones of nitrogen annually<sup>3</sup> and thus occupy a central position in nutrient recycling of ecosystems. With the severe desertification in some countries and regions, the strategy of utilization of cyanobacteria to reconstruct the soil ecosystem function has been widely proposed.<sup>4–6</sup>

*Nostoc flagelliforme* is a terrestrial, macroscopic, filamentous nitrogen-fixing cyanobacterium with great food and herbal value, which is distributed in the northern and north-western parts of China.<sup>7</sup> The habitats of *N. flagelliforme* are

characterized by conditions such as intense solar radiation, high temperature, alkali and extreme desiccation.<sup>8–10</sup> It has been suggested as pioneer organism in the desert due to the good adaptability to the extremes of living conditions. Additionally, *N. flagelliforme* can form biological crusts on the sand, which can change the nutrient composition and water conduction ability of the sand and ultimately affect the distribution of vegetation.<sup>11,12</sup> The biological crust can also adhere to sand granules and maintain soil moisture, which is important to enrich soil fertility. While the overexploitation of *N. flagelliforme* resources owing to ever-increasing market demand had resulted in serious damage to vegetation in its growing areas and the deterioration of the environment, causing more frequent sandstorms.<sup>13</sup> Therefore, *N. flagelliforme* is an essential part of soil ecosystem and play a significant role in sustainable development in ecosystem.

Like all photosynthetic organisms, cyanobacteria depend on solar radiation as their primary source of energy. UV-B radiation is a highly active component of the solar radiation that greatly affects the general physiology, biochemistry and redox status of the cell.<sup>14–16</sup> During the course of evolution, cyanobacteria have developed a number of defense strategies to counteract the damaging effects of UV-induced damages.<sup>17</sup>

Key Laboratory of Industrial Fermentation Microbiology, Ministry of Education, State Key Laboratory of Food Nutrition and Safety, College of Biotechnology, Tianjin University of Science and Technology, Tianjin 300457, P. R. China. E-mail: pphan@tust.edu.cn; Fax: +86 22 60602298; Tel: +86 22 60601598

† Electronic supplementary information (ESI) available. See DOI: 10.1039/c8ra04024a



Importantly, UV radiation induces the synthesis of mycosporine-like amino acids (MAAs) and scytonemin to protect cyanobacteria against harmful effects. MAAs are prominent photoprotectants that act against UV-B radiation. In addition, photosynthetic pigments play an important role in absorption and conversion of light energy, which have been reported to be adversely affected by UV-B radiation.<sup>18</sup> It was reported that reducing the ratio of photosynthetic pigments could increase the activity of photosynthesis and reduce photoinhibition at high light intensity.<sup>19</sup> Although there are a number of studies that have been carried out on the ecology, physiology, and culture of *N. flagelliforme*,<sup>20</sup> its UV-B tolerance and adaptation mechanisms are still not well understood. Besides, more physiological information related to the dynamic changes of cellular metabolism under UV-B radiation is required to understand its growth in nature. Because illustrating the responsive mechanism of *N. flagelliforme* to the UV-B radiation is of great importance for applying this organism to control desertification. Therefore, the present study intended to explore the physiological responses of *N. flagelliforme* to UV-B radiation. Three intensities of UV-B radiation (1, 3 and 5 W m<sup>-2</sup>) were used. The photosynthetic pigment, cell morphology, MAAs and cellular metabolism were comprehensively examined to study the UV-B adaptation mechanisms.

## 2. Materials and methods

### 2.1 Strains and experimental conditions

The *N. flagelliforme* was collected from the eastern side of the Helan Mountain in Yinchuan, Ningxia Hui Autonomous Region in China and stored in dry conditions at room temperature for 24 months before being used in experiments. The dissociated cells were obtained according to the methods described previously<sup>21</sup> and were cultured in BG-11 medium in air conditioned culture room at 25 ± 1 °C under cool-white fluorescent light at 60 μmol photons m<sup>-2</sup> s<sup>-1</sup>.

According to the reported results,<sup>22</sup> the ultraviolet radiation in Yinchuan shows seasonal changes and the intensity of UV-B radiation varies between 0.67 W m<sup>-2</sup> (winter) and 5.33 W m<sup>-2</sup> (summer). Therefore, the UV-B irradiation intensities applied in our experiment were set as 1, 3 and 5 W m<sup>-2</sup>.

Before the experiment, cells were firstly incubated in the dark room for 3 days, in order to reduce the stored compound and avoid the influence of white light from pre-culture. After that, the cells (of 0.5 absorbance at 750 nm) were placed in a 90 mm open sterile Petri dishes containing 15 mL medium. These Petri dishes were kept on a shaking incubator with low shaking speed set at 75 rpm in order to reduce the cell sedimentation and also to insure uniform exposure and then cells were irradiated with three intensities (1, 3 and 5 W m<sup>-2</sup>) of UV-B. The wavelength of ultraviolet lamp (Nanjing Huaqiang Electronic Co. LTD, China) used in the study was 280–300 nm. The UV meter (Sentry Optronics Co. Ltd, China) was used to measure the light intensity emitted by the UV lamp. The cells grown under white fluorescent light were treated as control.

### 2.2 The measurement of photosynthetic pigment

The measurement of photosynthetic pigments was performed according to the previously reported method.<sup>23</sup>

### 2.3 The observation of cell morphology

The morphology of cells was observed by the scanning electron microscope (SEM) (HITACHI SU-1510, Japan). The lyophilised cells were fixed to the scanning electron microscopic stubs with double-sided tape. The samples were then coated with a layer of gold, ~10 nm thick. The samples were observed in a SEM; accelerated voltage was operated at 15.0 kV.

### 2.4 Extraction of the MAAs

About 0.5 g of frozen cells was homogenized and MAAs were extracted with 5 mL 100% high-performance liquid chromatography (HPLC) grade methanol at 4 °C for 24 h. The aliquots were centrifuged (4000 × *g* for 10 min) and supernatants were evaporated to dryness at 45 °C in a vacuum evaporator. The above residues were resuspended in 0.5 mL ultra-pure water and few drops of chloroform were added to this solution and centrifuged to separate the lipophilic photosynthetic pigments from water-soluble MAAs. Thereafter, the aqueous phase passed through a 0.2 μm membrane filter prior to analysis.

### 2.5 Analyses of the MAAs

Further analysis of these partially purified aqueous solutions was carried out on an Agilent HPLC system (1100 Series) with quaternary pump, UV-Vis detector (photodiode array detector) and fitted with a Venusil XBP-C18 column (3 μm, 100 × 2.1 mm). The mobile phase A and B were 0.1% formic acid (v/v) in methanol and H<sub>2</sub>O, respectively. The elution used a mixture of 98% mobile phase A and 2% phase B from 0 to 9 min, 70% A + 30% B from 9 to 17 min, and 98% A + 2% B from 17 to 22 min, with flow rate of 1.0 mL min<sup>-1</sup> and column temperature set at 25 °C. The injection volume was 10 μL. Peaks were detected at 330 nm and absorption spectra were recorded from 300 to 400 nm for preliminary identification of compounds in the absence of commercially available standards.<sup>24</sup>

Then accurate mass measurement of MAAs were performed on IP-RPLC (ion-pair reversed-phase liquid chromatography) coupled to Q-TOF-MS (quadrupole time-of-flight mass spectrometry) equipped with a reversed phase symmetry C18 column 3.5 μm, 100 × 2.1 mm i.d. (Waters, Dublin, Ireland). The mobile phase and gradient elution were performed as above. The flow rate was set to 0.2 mL min<sup>-1</sup>, and 5 μL of sample was injected into the column. MS analysis of the samples was performed using micrOTOF-Q II mass spectrometer of Bruker Daltonik (Bremen, Germany). The electrospray ionization parameters were operated in positive ion mode, and mass spectra was recorded in the range *m/z* 50–1000. The capillary voltage was maintained at 2600 V with the end plate offset at –500 V. Nitrogen was used as nebulizer and dry gas at flow rate of 6.0 and 0.8 min L<sup>-1</sup>, respectively; source temperature was maintained at 180 °C.

Finally, MAAs mass spectral fragments analysis was performed on a Finnigan LC-ESI-MS<sup>n</sup> system consisting of a Surveyor HPLC with quaternary gradient pumps and an autosampler coupled with Finnigan LCQ Advantage ion-trap mass spectrometry (Thermo Electron, San Jose, CA, USA). A Venusil XBP-C18 column (5  $\mu\text{m}$ , 150 mm  $\times$  2.1 mm i.d.) was utilized for chromatographic separation. The LC flow was 0.2 mL min<sup>-1</sup>. The mobile phase and gradient elution were performed as above. The MS<sup>1</sup>/MS<sup>2</sup> analyses were carried out in positive ESI ionization mode. The product ions information was acquired by MS<sup>2</sup> scanning. Spray voltage was 5 kV and ion transfer capillary temperature was 300 °C. Nitrogen was used as sheath and auxiliary gases with flow rates set at 35 and 5 units, respectively. The normalized collision energy (CE) was 30%. The mass ranged from  $m/z$  50 to 1000 Dalton.

The relative content of MAAs in extract from cells was defined as peak area of MAAs per g dry cell weight by IP-RPLC-Q-TOF-MS.

## 2.6 Metabolite extraction and gas chromatography-mass spectrometry (GC-MS) analysis

The metabolite extraction and GC-MS analysis were performed according to the previously reported method.<sup>25</sup>

## 2.7 Statistics analysis

To ensure reproducibility of results, each experiment was performed at least three replications and the values are expressed as the mean  $\pm$  standard deviation. Missing values were replaced by the lowest value of the respective metabolite in the data set  $\pm$ 40% random variation to keep the variance of the data set. Principal component analysis (PCA) was performed by SIMCA package (ver. 11.5) (Umetrics, Umea, Sweden). The relative abundances of metabolites were standardized by mean 0 and variance 1 to generate a heat map by use of Expander 4.1 software (Expression Analyzer and DisplayER).

## 3. Results

### 3.1 Effects of UV-B radiation on the photosynthetic pigments

As shown in Fig. 1A–C, *N. flagelliforme* was sensitive to the changes of UV-B intensity and significant difference in photosynthetic pigments was observed. Compared to the control, the phycocyanin (PC) and allophycocyanin (APC) contents were increased in the first 6 h, and then greatly decreased from 6 h to 48 h, and their reductions were positively correlated with

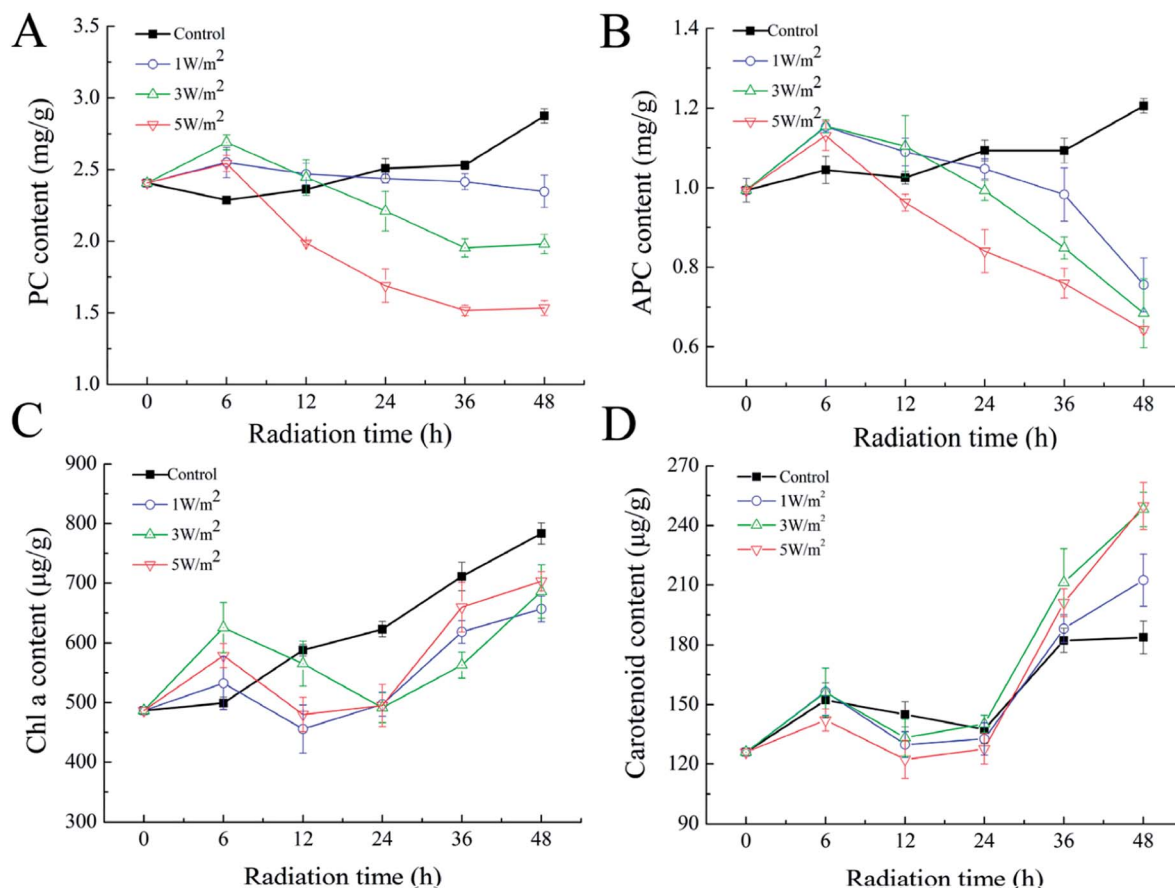


Fig. 1 Effects of UV-B radiation on the PC (A), APC (B), Chl a (C) and carotenoids (D) of *N. flagelliforme*.

**Table 1** Changes of the ratio of carotenoid to Chl *a* in the *N. flagelliforme* under different intensities of UV-B radiation for 48 h

UV-B treatment	Control	1 W m <sup>-2</sup>	3 W m <sup>-2</sup>	5 W m <sup>-2</sup>
Ratio of carotenoid/Chl <i>a</i>	0.23 ± 0.02	0.32 ± 0.01	0.35 ± 0.02	0.36 ± 0.02

radiation intensity, which was respectively decreased by 18.12%, 31.01%, 46.69% and 37.19%, 43.80%, 50.41% under 1 W m<sup>-2</sup>, 3 W m<sup>-2</sup> and 5 W m<sup>-2</sup> radiation (Fig. 1A and B). In addition, under all the UV-B radiation treatments, there was an initial increase in chlorophyll *a* (Chl *a*) content in comparison to the control in the first 6 h, followed by a rapid decrease from 6 h to 24 h, and then increased from 24 h to 48 h, but their contents were still lower than those of the control (Fig. 1C). As for carotenoids, its variation trend was similar to that of Chl *a*, but their contents were higher than that of the control, which were increased by 15.66%, 35.99% and 35.07% under 1 W m<sup>-2</sup>, 3 W m<sup>-2</sup> and 5 W m<sup>-2</sup> radiation, respectively (Fig. 1D).

Interestingly, the pigmentation of cells exposed to 3 W m<sup>-2</sup> and 5 W m<sup>-2</sup> of UV-B radiations changed from green to yellow (ESI Fig. S1†). This phenomenon might be due to an increase in the ratio of carotenoid/Chl *a*, as previously reported in the cyanobacteria *Synechococcus* and *Prochlorococcus*.<sup>26</sup> Therefore, the ratio of carotenoid to Chl *a* after 48 h of exposure were calculated. As depicted in Table 1, UV-B radiation had strong influence on the ratio of carotenoid to Chl *a*, and the ratio of carotenoid to Chl *a* was increased with the increase of UV-B intensity.

### 3.2 Observation of cell morphology by SEM

As shown in Fig. 2, under white light, SEM observations showed that the *N. flagelliforme* cells had smooth surface, round shape with similar size, intact plasmodesmata and the cells arranged in chains. Under 1 W m<sup>-2</sup> radiation for a short time (less than 12 h), the cell surface began to appear wrinkles, plasmodesmata fractured and subsequent duration of treatment (more than 24 h) resulting in depressions in the cell surface, even caused cells clumped together. While under 3 W m<sup>-2</sup> and 5 W m<sup>-2</sup> radiation for 6 h, the cell surface began to appear wrinkles and depression, and there were more wrinkles and larger depressions with the increase of radiation time. In addition, 5 W m<sup>-2</sup> radiation induced synthesis of a large number of viscous substances around cells, which made cell aggregation more obvious.

### 3.3 Identification and quantification of the MAAs

The UV scanning results of MAAs extract (Fig. 3A) showed absorbance peak in the UV spectrum ranged from 300–350 nm, which was consistent with literature reports. The identification of MAAs were based on accurate mass measurement of the molecular ions by IP-RPLC-Q-TOF-MS (Table 2) and detection of the product ions yielded from molecular ions by LC-ESI-MS<sup>n</sup> (ESI Fig. S2†). Three kinds of MAAs were identified including shinorine, asterina-330 and porphyra-334 according to the procedures.

From Fig. 3B, under 1 W m<sup>-2</sup> and 3 W m<sup>-2</sup> radiation, the porphyra-334 content was increased rapidly from 24 h to 48 h, which was 2.10-fold and 1.98-fold of the control, respectively. The highest porphyra-334 content was achieved under 5 W m<sup>-2</sup> radiation for 6 h, which was 2.82-fold of the control, then showed a sharp decrease from 6 h to 12 h, and eventually kept stable. As shown in Fig. 3C, under 1 W m<sup>-2</sup> radiation for 48 h, the shinorine content was 1.40-fold of the control; under 3 W m<sup>-2</sup>, the shinorine content showed a sharp increase from 24 h to 36 h, which was 2.89-fold of the control, then showed a sharp decrease. However, the shinorine content was greatly decreased under 5 W m<sup>-2</sup> radiation for 6 h, then rapidly increased from 6 h to 24 h, and eventually decreased from 24 h to 48 h. As for asterina-330, in the first 24 h of UV-B exposure at 1 W m<sup>-2</sup>, 3 W m<sup>-2</sup> and 5 W m<sup>-2</sup>, there was no significant change in their contents, while after 48 h, the increase in asterina-330 content was 2.52-fold, 2.31-fold and 4.42-fold to that of the control, respectively (Fig. 3D). The total contents of two (asterina-330 and shinorine) and three kinds of MAAs in cells were calculated, which was shown in panel E and F in Fig. 3. Interestingly, with the increase of radiation time, their variation trend was similar.

### 3.4 Metabolism of *N. flagelliforme* under UV-B exposure

A total of 65 metabolic compounds, with 60 of the putatively identified (comprised 14 organic acids, 9 amino acids, 16 sugars, 4 alcohols, 16 fatty acids and 1 ester), was quantified by GC-MS (ESI Table S1†). The overview of the metabolite profiles of *N. flagelliforme* cells under different intensities of UV-B treatment by metabolic heat map analysis was presented in Fig. 4A. As shown in Fig. 4A, the intracellular metabolism was greatly affected by the UV-B radiation and most of the metabolites were reduced under all the UV-B treatments. Besides that, the change patterns of metabolites under different UV-B treatments were various. PCA was used to obtain a global comparison of metabolite profiles of *N. flagelliforme* under different intensities of UV-B. In the PCA score plot  $t[1]/t[2]$  (Fig. 4B), control sample were located in the upper left quadrant; samples from cells under 3 W m<sup>-2</sup> and 5 W m<sup>-2</sup> radiation clustered together, while cells under 1 W m<sup>-2</sup> radiation were clearly separated from them and located in the right quadrant.

To illustrate the influence of UV-B on metabolism, the variations of measured metabolites were mapped onto the biosynthetic pathways as shown in Fig. 5. According to the metabolic network diagram, these metabolites divided into three categories of metabolism: starch metabolism, amino acid metabolism and fatty acid metabolism. From Fig. 5, compared with the control, the metabolism of cells under different intensities of UV-B was significantly changed. In terms of starch metabolism, under all the UV-B treatments, the glucose content was increased in the first 12 h, and the increase was positively correlated with UV-B intensity, followed by a decrease from 12 h to 48 h. Under 3 W m<sup>-2</sup> and 5 W m<sup>-2</sup> radiation for 12 h, the glucose content was much higher than that of the control. In addition, UV-B radiation at 1 W m<sup>-2</sup> greatly promoted the sucrose synthesis, while UV-B radiation at 5 W m<sup>-2</sup> significantly

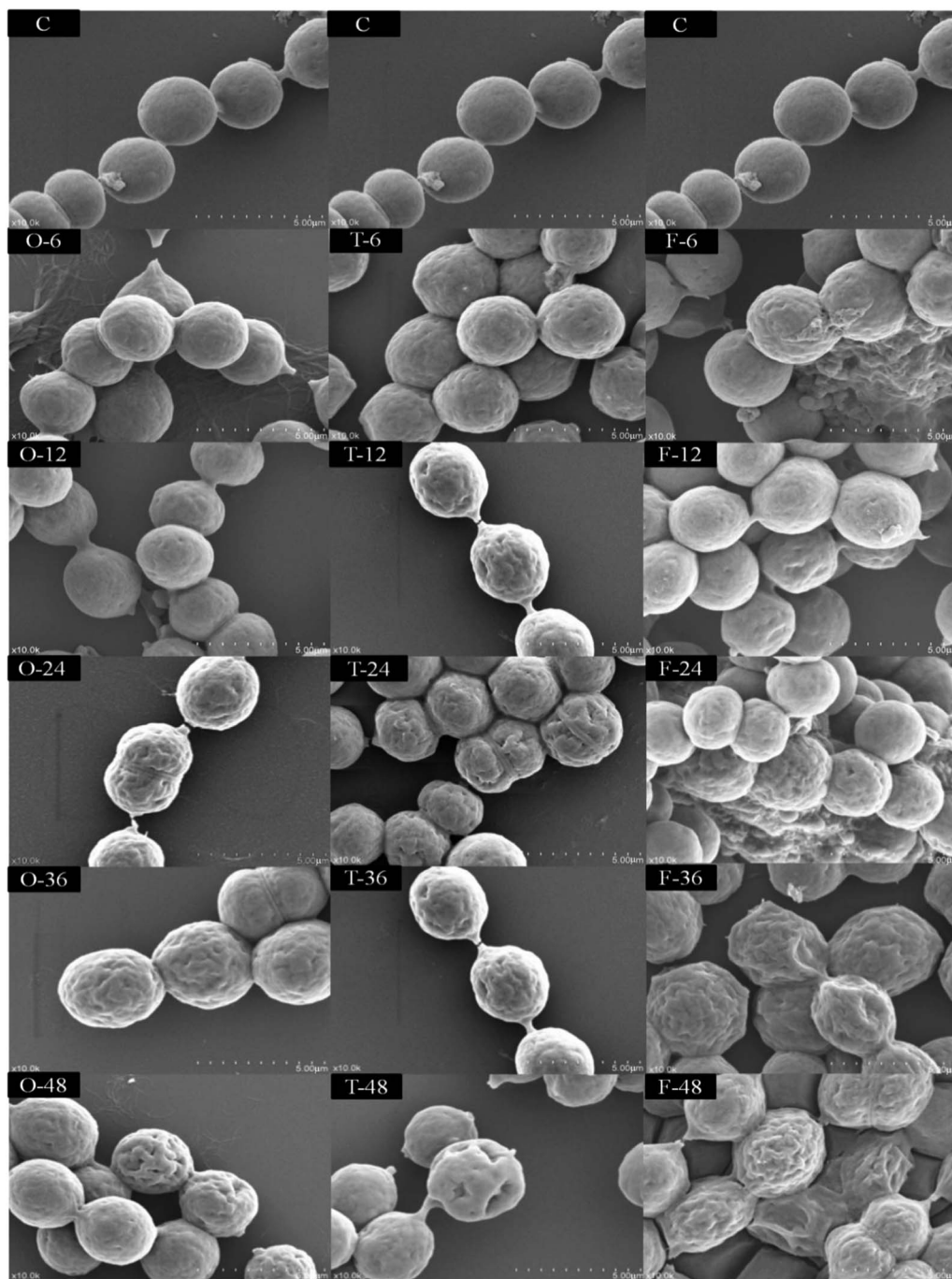


Fig. 2 Morphology of cells exposed to different intensities of UV-B radiation. C stands for the control group, the letter O, T and F in the upper left represented the  $1 \text{ W m}^{-2}$ ,  $3 \text{ W m}^{-2}$  and  $5 \text{ W m}^{-2}$  radiation and the number stands for the UV-B radiation time. Bars indicate  $5 \mu\text{m}$ .

increased the mannitol content. Under whatever the UV-B intensity, the contents of valine and serine were greatly decreased, while the glycine, threonine and proline accumulated higher amounts, especially under  $3 \text{ W m}^{-2}$  and  $5 \text{ W m}^{-2}$  radiation. As shown in Fig. 5, fatty acid was sensitive to the changes of UV-B intensity and significant difference in the content was observed. In terms of saturated fatty acids, under all the UV-B treatments, the variation trend of octadecanoic acid was similar to that of palmitic acid. Under  $1 \text{ W m}^{-2}$  radiation,

the saturated fatty acid content was increased with the increase of radiation time, and the content was much higher than that of the control; under  $3 \text{ W m}^{-2}$  and  $5 \text{ W m}^{-2}$  radiation, it was firstly increased from 0 to 12 h and then decreased from 24 h to 48 h, but their contents were still higher than that of the control. As for unsaturated fatty acid, compared to the control, the unsaturated fatty acids content was greatly reduced under all the UV-B treatments, except the eicosenoic acid, which was significantly higher under  $3 \text{ W m}^{-2}$  radiation than that of the control.

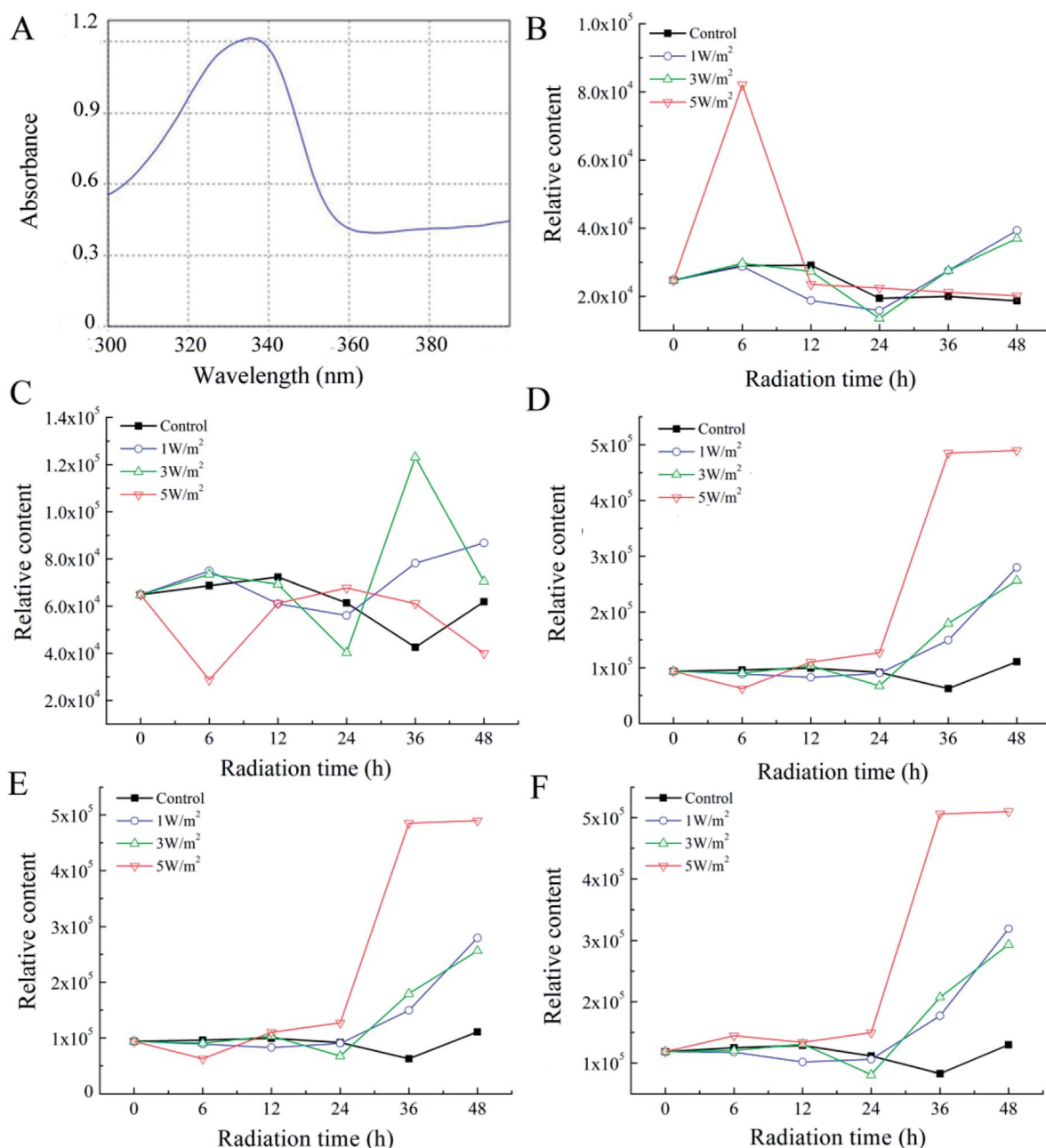


Fig. 3 The identification and quantification of MAAs existed in cells of *N. flagelliforme* under UV-B radiation. The absorption spectra of MAAs were shown in panel (A). The relative contents of porphyra-334 (B), shinorine (C), asterina-330 (D), both asterina-330 and shinorine (E) and total MAAs (F) in cells upon exposure to UV-B radiation.

Table 2 Observed masses of MAAs by IP-RPLC-Q-TOF-MS

	Retention time (min)	Observed $m/z$ value ( $[M + H]^+$ )	Calculated $m/z$ value ( $[M + H]^+$ )	Error (ppm)	Formula
Asterina-330	3.0	289.1395	289.1400	-0.7	$C_{12}H_{19}N_2O_6$
Shinorine	1.7	333.1297	333.1298	-0.3	$C_{13}H_{21}N_2O_8$
Porphyra-334	2.2	347.1454	347.1454	0	$C_{14}H_{22}N_2O_8$

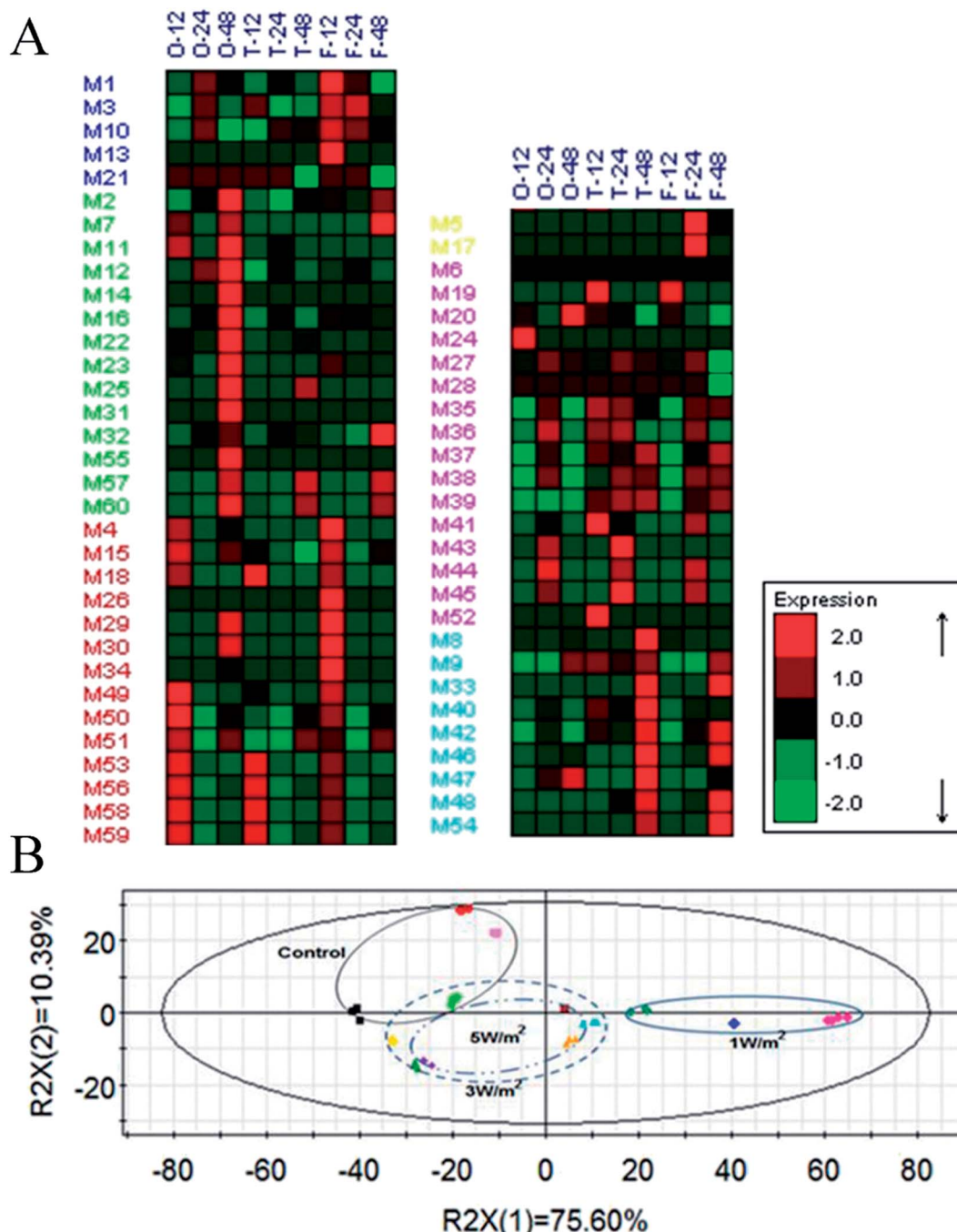


Fig. 4 A metabolic heat map that summarizes the differences in metabolite variations of *N. flagelliforme* under different UV-B intensity (A). The letter O, T and F in the upper left represented the  $1 \text{ W m}^{-2}$ ,  $3 \text{ W m}^{-2}$  and  $5 \text{ W m}^{-2}$  radiation and the number stands for the UV-B radiation time. The PCA score plot of the metabolites analyzed in *N. flagelliforme* under different UV-B intensity (B).

## 4. Discussion

With the aggravation of desertification in some countries and regions, the application of cyanobacteria to reconstruct the soil ecosystem function has been studied extensively in recent years. Our previous study showed that liquid suspension-cultured *N. flagelliforme* cells could grow on sands and form soil crusts under laboratory conditions.<sup>5</sup> However, the adaptability and response mechanism to UV-B radiation have not been fully

explored yet. In this study, effects of different intensities of UV-B radiation on the photosynthetic pigment, cell morphology, MAAs and cellular metabolism were comprehensively investigated.

In the first 6 h of UV-B radiation, the content of PC, APC and Chl *a* was increased compared to the control, which might be due to short term of the radiation stimulated protective responses that affect the resistance to UV-B stress, and thus promoted the synthesis of photosynthetic pigments. Longer UV-

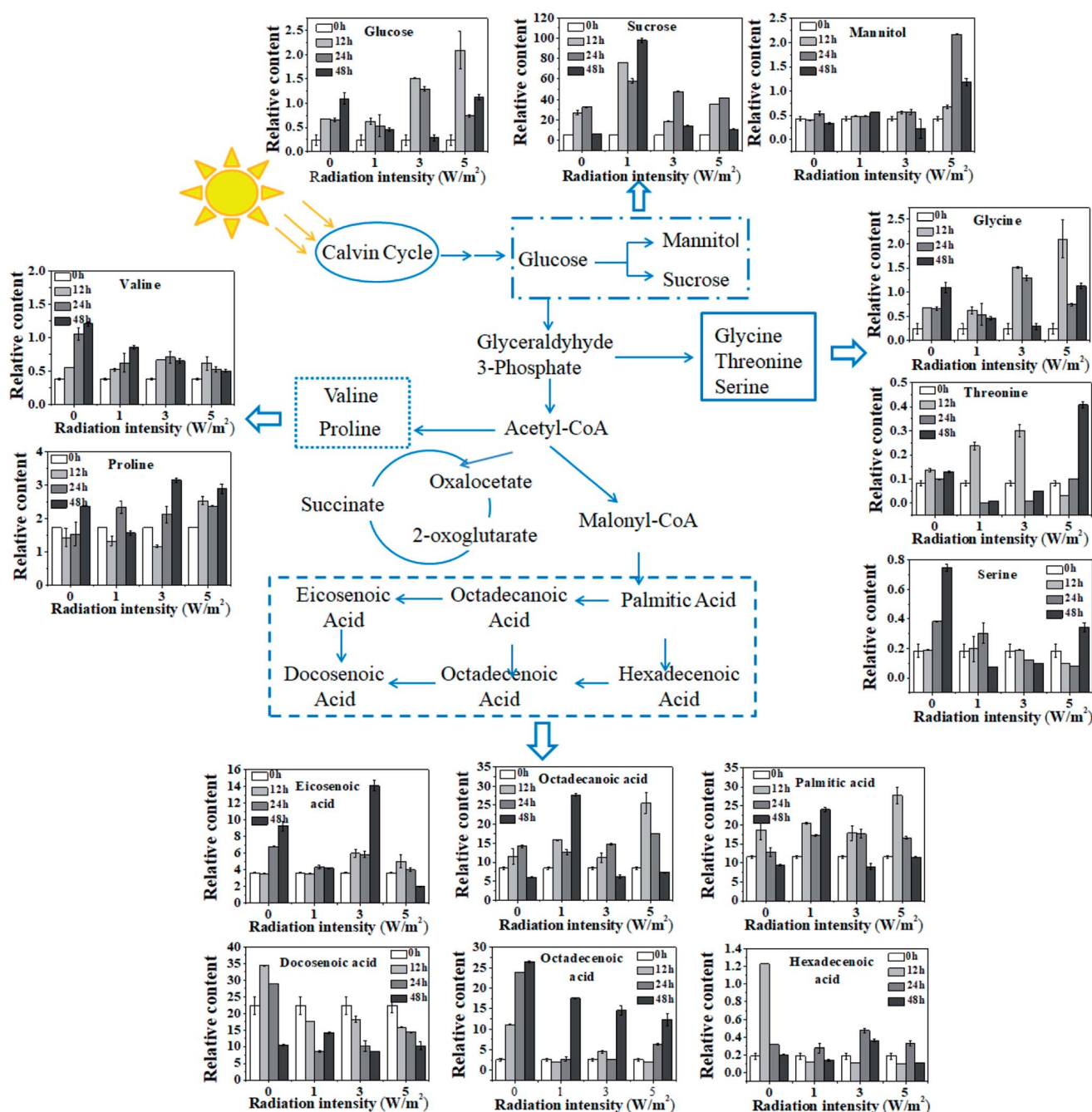


Fig. 5 Variations of metabolite abundance in *N. flagelliforme* under different intensities of UV-B.

B treatment time (more than 6 h) reduced the contents of PC, APC and Chl *a*, but the radiation intensity reduced more, indicating that long term of the exposure caused damage on the photosynthetic apparatus, and the UV-B intensity had greater damage than exposure time (Fig. 1A-C). Compared to Chl *a*, PC and APC were severely affected. That was because UV-B interacted with PC and APC directly, and PC and APC localized on the outer surface of thylakoid membrane.<sup>27</sup> There are some reports that the damaging effect on PC, APC and Chl *a* is due to the bleaching caused by UV-B radiation or through reactive

oxygen species (ROS) mediated peroxidation.<sup>28-30</sup> Li *et al.* also reported that UV-B radiation could indirectly generate ROS at multiple sites of the photosynthetic electron transport chain in cyanobacteria and had great damage on the photosynthetic pigments.<sup>31</sup> The decrease of Chl *a* content may be a strategy for adaptation to prevent overexcitation in the reaction center.<sup>32</sup> The increase in carotenoid contents in response to UV-B radiation may be attributed to its protective role in scavenger of ROS.<sup>33,34</sup> In addition, the ratio of carotenoid/Chl *a* was a marker indicating cellular oxidative level,<sup>35</sup> which indicated that 3 W m<sup>-2</sup>



and  $5 \text{ W m}^{-2}$  radiation might induce a large amount of ROS and thus stimulated the formation of carotenoid to protect cells from ROS.

In addition to synthesize a large number of carotenoid, as the earliest photosynthetic organism, cyanobacteria have evolved other defense strategies that allow them to survive and grow in adverse environments with high UV-B intensity, including avoidance and synthesis of UV-absorbing/screening compounds<sup>36</sup> and so on.

As the first line of defense against the elevated UV-B in their natural habitats, a number of cyanobacteria have developed avoidance mechanisms, such as mat formation and morphological transformation. SEM observations showed that when cells exposed under UV-B radiation for a short time (less than 12 h), cell surface began to appear wrinkles, and plasmodesmata fractured and long term of exposure (more than 24 h) resulted in depressions in the cell surface, even caused cells clumped together (Fig. 2). This phenomenon is similar to the morphological changes of *A. germinans*,<sup>37</sup> and it is more pronounced under  $5 \text{ W m}^{-2}$  radiation. In addition, under  $5 \text{ W m}^{-2}$  radiation, the cells appear to be more compact, resulting in self shading, and this is also an effective protective mechanism against UV-B.<sup>38</sup> Compared to aquatic systems, terrestrial habitats are more favorable for mat formation because of periodic long-term desiccation and higher UV-B.<sup>39</sup> Although cells are unable to form crust or mat in liquid environment, the cell surface is covered with mucous substance, making the cell density larger, which favors the cell sink to the bottom of water to escape high UV-B intensity.

Photoprotective compounds play an important role in screening UV-B radiation in cyanobacteria and it is an important line of defense.<sup>40</sup> MAAs and scytonemin are prominent photoprotective compounds that act against UV-B and/or UV-A radiation. As shown in Fig. 3, three kinds of MAAs were detected in the control group, suggesting the *N. flagelliforme* cells could synthesize MAAs even if not illuminated with UV-B. For the UV-B treatments, the contents of three kinds of MAAs were increased to some extent, but their variation trends were different. It is reported that MAAs could transform from one to another through addition or deletion of amino acids and some groups *in vivo*.<sup>41,42</sup> According to the transformation relationship among MAAs, it is obvious that asterine-330 is located downstream of shinorine, and it is the final product of shinorine. Besides that, porphyra-334 and shinorine are two different downstream branches of the same precursor, and they should belong to the competitive relationship. When cells exposed to  $1 \text{ W m}^{-2}$  radiation, they synthesized a small amount of shinorine and porphyra-334 against UV-B. However, when shinorine and porphyra-334 could not eliminate the damage caused by the increasing UV-B intensity, more shinorine turned into asterine-330. The induction of MAAs under different intensities of UV-B appeared to be uneven. It could be concluded that the metabolic flux had already changed in terms of MAAs under different intensities of UV-B, and asterine-330 might be the most effective MAAs against UV-B.

In order to fully explore the responsive mechanism of *N. flagelliforme* to the UV-B radiation, it is necessary to investigate the dynamic changes of cellular metabolism under UV-B

radiation. Therefore, a metabolic profiling approach was employed to provide an overview of the metabolite profiles of *N. flagelliforme* under different intensities of UV-B. The metabolic heat map showed that the change patterns of metabolites under different UV-B treatments were various, which confirmed the different sensitivity of *N. flagelliforme* cells to the UV-B intensity and/or radiation time (Fig. 4A). Besides that, the discrimination on the PCA profile reflected the metabolic difference caused by UV-B intensity and it also indicated that the influence was intensity specific (Fig. 4B). Under all UV-B treatments, the content of most metabolites increased significantly (Fig. 5). Of these metabolites, the relative content of sucrose is the highest, especially under  $1 \text{ W m}^{-2}$  radiation after 48 h, which is 15.66-fold of the control. Sucrose, as a soluble sugar, has important role in carbohydrate storage and stress responses.<sup>43</sup> In addition, under  $5 \text{ W m}^{-2}$  radiation, the cells accumulated large amounts of mannitol. Mannitol has been correlated with stress tolerance in several plants species,<sup>44</sup> which is implicated in stabilizing macromolecules and scavenging hydroxyl radicals, therefore preventing oxidative damage of membranes and enzymes.<sup>45,46</sup> Similar to sucrose, some amino acids in microbial cells also play important roles in stress tolerance,<sup>47</sup> especially proline, which is considered to act as an osmolyte, a ROS scavenger, and a molecular chaperone stabilizing the structure of proteins.<sup>48,49</sup> In fatty acid metabolism, overall, UV-B radiation promoted the saturated fatty acid accumulation, but inhibited the unsaturated fatty acid. Saturated fatty acid provides the energy required for rebuilding of the photosynthetic apparatus. Unsaturated fatty acid is known in regulating membrane fluidity and physiological processes under stress and membrane lipid unsaturation increases the tolerance of cyanobacterium to UV radiation.<sup>50,51</sup> Combined with the above results, it seems reasonable to suggest that high UV-B radiation ( $3 \text{ W m}^{-2}$  and  $5 \text{ W m}^{-2}$ ) may cause the cell membrane disruption, thus greatly promotes the accumulation of carotenoids, MAAs and intracellular cytoprotective metabolites, such as sucrose and proline.

## 5. Conclusion

In this study, the effects of different intensities of UV-B on photosynthetic pigment, cell morphology, MAAs production, and cell metabolism were comprehensively investigated. It was found that *N. flagelliforme* cells exhibited different degrees of sensitivity to UV-B radiation and the UV-B intensity had greater damage on cells than exposure time. The damage to cells mainly reflected on the decrease of Chl *a*, PC and APC content, changes of cell morphology, and fatty acid metabolism. To adapt to the stress, under  $1 \text{ W m}^{-2}$  radiation, cells synthesized a large number of sucrose to counteract UV-B radiation damage, but when the radiation intensity increased to  $3 \text{ W m}^{-2}$ , cells synthesized many carotenoids and cytoprotective metabolites, such as sucrose, proline and glucose. While under  $5 \text{ W m}^{-2}$  radiation, cells synthesized a large number of MAAs and mannitol to counteract UV-B radiation damage. The findings would improve the understanding of physiological responses of *N. flagelliforme* to UV-B radiation. Based on this study, proper shading to reduce the

radiation intensity is very helpful to cultivate the *N. flagelliforme* in outdoor to control desertification in the future.

## Conflicts of interest

There are no conflicts to declare.

## Acknowledgements

The authors are very grateful for the financial support from the National Natural Science Foundation of China (Grant No. 31671842) and Changjiang Scholars and Innovative Research Team in University (Grant No. IRT1166).

## References

- 1 W. W. Fischer, *Nature*, 2008, **455**, 1051–1052.
- 2 I. Berman-Frank, P. Lundgren and P. Falkowski, *Res. Microbiol.*, 2003, **154**, 157–164.
- 3 M. Koller, A. Muhr and G. Brauneegg, *Algal Res.*, 2014, **6**, 52–63.
- 4 M. J. Acea, N. Diz and A. Prieto-Fernández, *Biol. Fertil. Soils*, 2001, **33**, 118–125.
- 5 X. F. Chen, S. R. Jia, Y. Wang and N. Wang, *J. Appl. Phycol.*, 2011, **23**, 67–71.
- 6 C. X. Hu and Y. D. Liu, *Acta Bot. Sin.*, 2003, **45**, 917–924.
- 7 K. S. Gao and D. G. Zou, *J. Appl. Phycol.*, 2001, **37**, 768–771.
- 8 W. K. Dodds, D. A. Gudder and D. Mollenhauer, *J. Phycol.*, 1995, **31**, 2–18.
- 9 P. P. Han, S. R. Jia, Y. Sun, Z. L. Tan, C. Zhong, Y. J. Dai, N. Tan and S. G. Shen, *World J. Microbiol. Biotechnol.*, 2014, **30**, 2407–2418.
- 10 K. X. Qian, H. R. Zhu and S. G. Chen, *Acta Phytoecologica et Geobotanica Sinca*, 1989, **13**, 97–105.
- 11 K. S. Gao, *J. Appl. Phycol.*, 1998, **10**, 37–49.
- 12 B. Don, P. M. Andrew and R. R. James, *J. Phycol.*, 1973, **9**, 99–101.
- 13 P. P. Han, S. G. Shen, S. R. Jia, H. Y. Wang, C. Zhong, Z. L. Tan and H. X. Lv, *World J. Microbiol. Biotechnol.*, 2015, **31**, 1061–1069.
- 14 K. S. Gao, J. T. Xu, G. Gao, Y. H. Li, D. A. Hutchins, B. Q. Huang, L. Wang, Y. Zheng, P. Jin, X. N. Cai, D. P. Häder, W. Li, K. Xu, N. N. Liu and U. Riebesell, *Nat. Clim. Change*, 2012, **2**, 519–523.
- 15 R. P. Rastogi, R. P. Sinha, S. H. Moh, T. K. Lee, S. Kottuparambil, Y. J. Kim, J. S. Rhee, E. M. Choi, M. T. Brown, D. P. Häder and T. Han, *J. Photochem. Photobiol., B*, 2014, **141**, 154–169.
- 16 R. P. Rastogi, R. R. Sonani and D. Madamwar, *Photochem. Photobiol.*, 2015, **91**, 837–844.
- 17 R. P. Rastogi and D. Madamwar, *Biochem. Anal. Biochem.*, 2015, **4**(2), 173, DOI: 10.4172/2161-1009.1000173.
- 18 J. F. Bornman, *J. Photochem. Photobiol., B*, 1989, **4**, 145–158.
- 19 A. Melis, J. Neidhardt and J. R. Benemann, *J. Appl. Phycol.*, 1999, **10**, 515–525.
- 20 B. S. Qiu and K. S. Gao, *Eur. J. Phycol.*, 2001, **36**(2), 147–156.
- 21 H. F. Yu, S. R. Jia and Y. J. Dai, *J. Appl. Phycol.*, 2009, **21**, 127–133.
- 22 H. F. Yu and R. Liu, *J. Appl. Phycol.*, 2013, **25**, 1441–1446.
- 23 P. P. Han, S. G. Shen, H. Y. Wang, S. Y. Yao, Z. L. Tan, C. Zhong and S. R. Jia, *J. Appl. Phycol.*, 2017, **29**, 55–65.
- 24 J. M. Shick and W. C. Dunlap, *Annu. Rev. Physiol.*, 2002, **64**, 223–262.
- 25 P. P. Han, Y. Sun, S. R. Jia, C. Zhong and Z. L. Tan, *Carbohydr. Polym.*, 2014, **105**, 145–151.
- 26 L. R. Moore, R. Goericke and S. W. Chisholm, *Mar. Ecol.: Prog. Ser.*, 1995, **116**, 259–275.
- 27 M. Zeeshan and S. M. Prasad, *S. Afr. J. Bot.*, 2009, **75**, 466–474.
- 28 W. Nultsch and G. Agel, *Arch. Microbiol.*, 1986, **144**, 268–271.
- 29 I. Vass, L. Sass, C. Spetea, A. Bakou, D. F. Ghanotakis and V. Petrouleas, *Biochemistry*, 1996, **35**, 8964–8973.
- 30 A. Latifi, M. Ruiz and C. C. Zhang, *FEMS Microbiol. Rev.*, 2009, **33**, 258–278.
- 31 Z. K. Li, G. Z. Dai, P. Juneau and B. S. Qiu, *J. Phycol.*, 2017, **53**(2), 425–436.
- 32 T. Han, R. P. Sinha and D. P. Häder, *Photochem. Photobiol. Sci.*, 2003, **2**, 649–654.
- 33 A. Quesada, J. L. Mouget and W. F. Vincent, *J. Phycol.*, 1995, **31**, 242–248.
- 34 E. M. Middleton and A. H. Teramura, *Plant Physiol.*, 1993, **103**, 741–752.
- 35 L. Schitüter, R. Bo and M. Søndergaard, *J. Plankton Res.*, 1997, **19**, 891–906.
- 36 K. S. Gao and C. P. Ye, *J. Phycol.*, 2007, **43**, 628–635.
- 37 R. P. Sheridan, *J. Phycol.*, 2001, **37**(5), 731–737.
- 38 H. Y. Wu, K. S. Gao, V. E. Villafañe, T. Watanabe and E. W. Helbling, *Appl. Environ. Microbiol.*, 2005, **71**, 5004–5013.
- 39 K. A. Hughes and B. Lawley, *Environ. Microbiol.*, 2003, **5**(7), 555–565.
- 40 S. P. Singh, D. P. Häder and R. P. Sinha, *Ageing Res. Rev.*, 2010, **9**, 79–90.
- 41 R. P. Sinha, S. P. Singh and D. P. Häder, *J. Photochem. Photobiol., B*, 2007, **89**(1), 29–35.
- 42 R. P. Rastogi, Richa, R. P. Sinha, S. P. Singh and D. P. Häder, *J. Ind. Microbiol. Biotechnol.*, 2010, **37**(6), 537–558.
- 43 J. Krasensky and C. Jonak, *J. Exp. Bot.*, 2012, **63**(4), 1593–1608.
- 44 J. H. M. Stoop, J. D. Williamson and D. M. Pharr, *Trends Plant Sci.*, 1996, **1**, 139–144.
- 45 N. Smirnoff and Q. J. Cumbes, *Phytochemistry*, 1989, **28**, 1057–1060.
- 46 B. Shen, R. G. Jensen and H. J. Bohnert, *Plant Physiol.*, 1997, **113**, 1177–1183.
- 47 H. Li, M. L. Ma, S. Luo, R. M. Zhang, P. Han and W. Hu, *Int. J. Biochem. Cell Biol.*, 2012, **44**, 1087–1096.
- 48 N. Verbruggen and C. Hermans, *Amino Acids*, 2008, **35**, 753–759.
- 49 L. Szabados and A. Savoure, *Trends Plant Sci.*, 2010, **15**, 89–97.
- 50 J. M. Hall, C. C. Parrish and R. J. Thompson, *Biol. Bull.*, 2002, **202**, 201–203.
- 51 S. M. Ehling and S. Scherer, *Eur. J. Phycol.*, 1999, **34**, 329–338.